

Application Note

A Study of the Analysis of Polybrominated Diphenyl Ether Flame Retardants by GC-MS/MS

Keith Worrall, Anthony Newton, Bert van Bavel, A. Pettersson, Gunilla Lindstrom, Eric J. Reiner, Karen MacPherson, Terry Kolic, Nicholas Ordsmith, S. Catterall, Keith Hall

Waters Corporation, MTM Research Centre, Örebro University, Ontario Ministry of the Environment and Climate Change, Hall Analytical Laboratories Ltd.

Abstract

The development of a GC-MS/MS method for the analysis of brominated flame retardants will be presented. Standard methods require the use of high resolution magnetic sector instrumentation, which can be costly and time consuming, requiring daily calibration across wide mass ranges. The use of GC triple quadrupole mass spectrometry removes the need for daily instrument calibration, whilst offering the analyst a high degree of selectivity by monitoring compound-specific fragmentation patterns. Three GC columns were assessed for both sensitivity and separation, with results presented for the most suitable column satisfying both criteria.

Benefits

GC triple quadrupole MS provides a sensitive and easy to apply method for the analysis of brominated diphenyl ether flame retardants, offering a rapid analysis time whilst providing suitable confirmation of analyte presence

Introduction

Polybrominated diphenyl ether (BDE) flame retardants have been of increasing concern to environmental analysts in recent years and have recently made front page news.¹ Current analytical techniques for BDE analysis generally involve the use of HR/GC-HR/MS, a costly technique requiring highly trained operators. Methods have also been published using single quadrupole GC-MS^{2,3} or GC-MS/MS (iontrap).⁴ The purpose of this study was to investigate the suitability of a GC triple-quadrupole instrument for the analysis of BDEs, monitoring compound-specific fragmentation patterns with the use of multiple reaction monitoring (MRM) acquisitions.

Experimental

All analyses were performed using an Agilent 6890 GC oven directly interfaced to a Waters Micromass Quattro micro GC Mass Spectrometer. The mass spectrometer was operated in EI+ mode for all analyses. GC analysis was performed on 30 m DB1-HT, 250 μm i.d., 0.1 μm film; 15 m DB1-HT, 250 μm i.d., 0.1 μm film and 20 m DB5-ms 180 μm i.d., 0.18 μm film GC Columns. All injections were made in splitless mode, using a 2 mm i.d. deactivated quartz injection liner with an injector temperature of 260 $^{\circ}\text{C}$.

The GC temperature ramps employed for all injections are as follows:

20 m DB5-ms: 140 $^{\circ}\text{C}$ /4 mins, 20 $^{\circ}\text{C}/\text{min}$ to 220 $^{\circ}\text{C}$, 30 $^{\circ}\text{C}/\text{min}$ to 315 $^{\circ}\text{C}$, hold 19 mins. He flow 0.6 mL/min, constant flow mode.

15 m DB1-HT: 140 $^{\circ}\text{C}$ /1 min, 10 $^{\circ}\text{C}/\text{min}$ to 220 $^{\circ}\text{C}$, 20 $^{\circ}\text{C}/\text{min}$ to 320 $^{\circ}\text{C}$, hold 3 mins. He flow 1 mL/min, constant flow mode.

30 m DB1-HT: 140 $^{\circ}\text{C}$ /2 mins, 5 $^{\circ}\text{C}/\text{min}$ to 220 $^{\circ}\text{C}$, 20 $^{\circ}\text{C}/\text{min}$ to 320 $^{\circ}\text{C}$, hold 7 mins. He flow 1 mL/min, constant flow mode.

Prior to analysis, the instrument was calibrated over the mass range 50–1200 Da using Tris(perfluoroheptyl)-1,3,5-triazine. Figure 1 presents a typical instrument mass calibration curve for this compound.

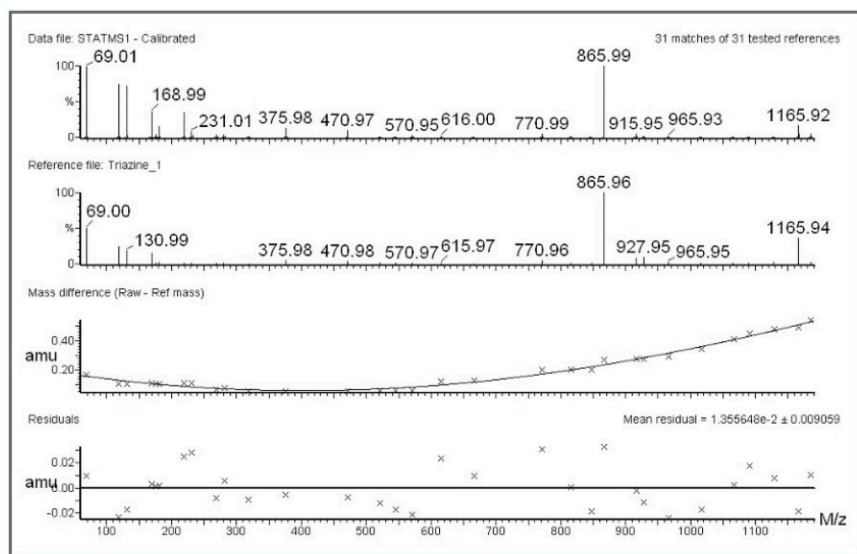


Figure 1. *Tris(perfluoroheptyl)-1,3,5-triazine* calibration curve.

Standards were acquired in full scan and precursor ion mode to investigate the most suitable transitions for MRM analysis. A five-point calibration curve, covering a total (congener specific) concentration range of 1–2000 pg on column was acquired in MRM mode, followed by solvent blank (nonane), sample extracts, solvent blank (nonane) and finally the BDE-CS3-E calibration standard as a QC check.

Results and Discussion

All PBDE congeners were identified by full scan GC-MS analysis, showing as major ions the $[M]^+$ or $[M-Br_2]^+$ isotopic cluster. Figure 2 shows the full scan mass spectra for the tetra brominated BDE#47 and Figure 3 shows the full scan mass spectra for the deca brominated BDE#209.

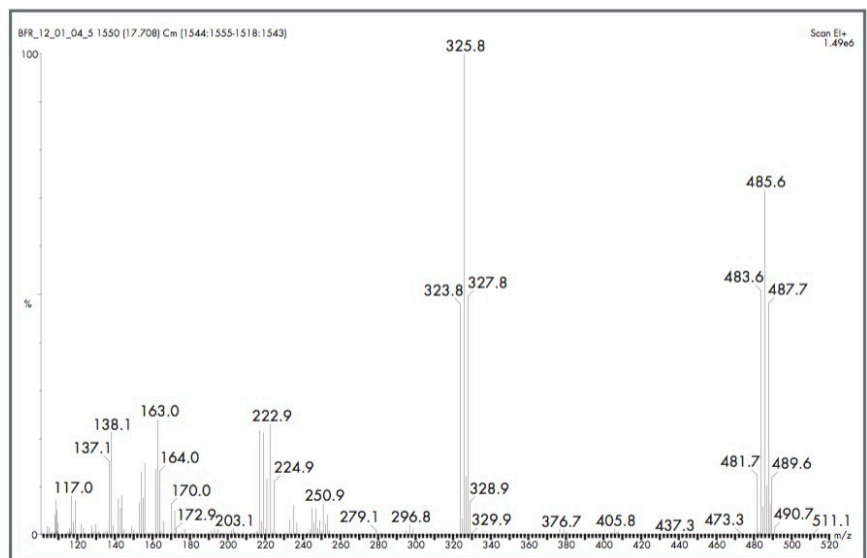


Figure 2. Full scan EI+ mass spectrum for BDE#47.

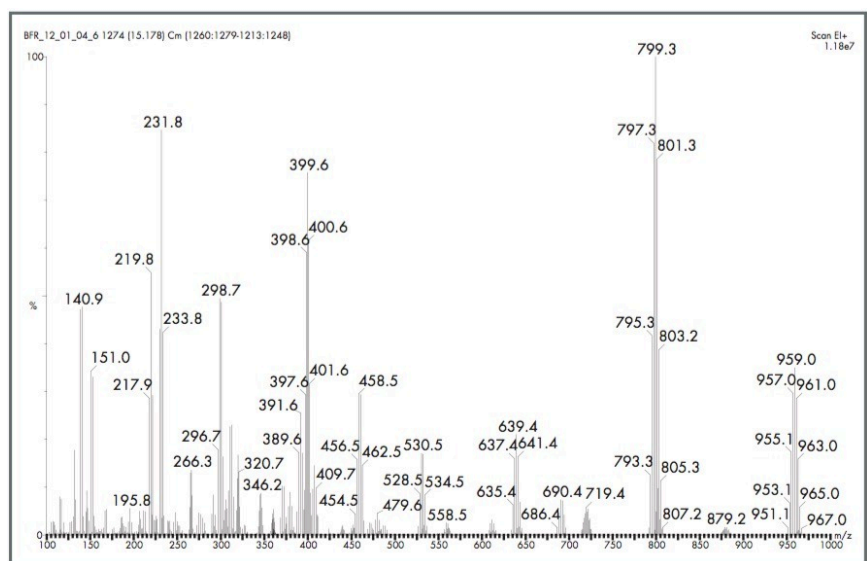


Figure 3. Full scan EI+ mass spectrum for BDE#209.

From the ions observed by full scan MS, the most abundant ions were selected for product ion scanning, generally one ion from the $[M]^+$ cluster and one ion from the $[M-Br_2]^+$ cluster, in order to achieve maximum sensitivity, but to also provide confirmatory ions. Figure 4 depicts the product scans for BDE#47, showing the

spectrum for the $[M]^+$ precursor ion.

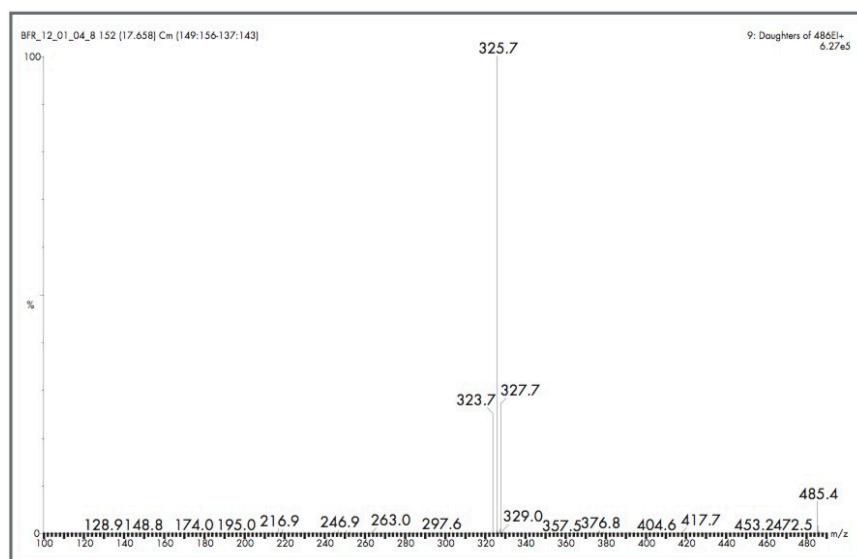


Figure 4. Product ion spectra for the precursor ion m/z 485.7 (M^+).

Table 1 shows the precursor ions, product ions, and optimal collision energies for each level of bromination from mono to deca bromo BDE.

| BDE | Precursor ion | Product ion | Collision energy(eV) |
|--------------------|----------------------------|---------------------------|----------------------|
| mono bromo | 248 [M] | 141 [-COBr] | 15 |
| | 250 [M] | 141 [-COBr] | 15 |
| di bromo | 327.9 [M] | 168.1 [-Br ₂] | 20 |
| | 168.1 [M-Br ₂] | 139 [-COH] | 20 |
| tri bromo | 407.8 [M] | 248 [-Br ₂] | 15 |
| | 248 [M-Br ₂] | 139 [-COBr] | 30 |
| tetra bromo | 485.7 [M] | 325.9 [-Br ₂] | 20 |
| | 325.9 [M-Br ₂] | 138 [-COBr ₂] | 45 |
| penta bromo | 565.6 [M] | 405.8 [-Br ₂] | 25 |
| | 403.8 [M-Br ₂] | 137 [-COBr ₃] | 55 |
| hexa bromo | 643.5 [M] | 483.7 [-Br ₂] | 20 |
| | 483.7 [M-Br ₂] | 374.8 [-COBr] | 30 |
| hepta bromo | 723.4 [M] | 563.6 [-Br ₂] | 25 |
| | 563.6 [M-Br ₂] | 454.7 [-COBr] | 30 |
| octa bromo | 801.3 [M] | 641.5 [-Br ₂] | 25 |
| | 641.5 [M-Br ₂] | 534.6 [-COBr] | 30 |
| nona bromo | 881.3 [M] | 719.4 [-Br ₂] | 25 |
| | 719.4 [M-Br ₂] | 612.5 [-COBr] | 35 |
| deca bromo | 959.2 [M] | 799.3 [-Br ₂] | 25 |
| | 799.3 [M-Br ₂] | 639.5 [-Br ₂] | 45 |

Table 1. Optimised precursor and product ions for mono to deca brominated diphenyl ethers.

Table 2 shows the precursor ions, product ions, and optimal collision energies for each level of bromination from mono to deca bromo BDE for the ¹³C₁₂ labelled internal standards. The transitions and collision energies from tables 1 & 2 were then used to create a 10 function MRM experiment, monitoring each level of bromination in single functions. To allow for possible retention time shifts of the first and last eluting congeners of some levels of bromination, the start and end time of functions 3,4,5,6,7 (tribromo to hepta-bromo) were overlapped (end time

of previous function after start time of current function).

| ¹³C-BDE | Precursor ion | Product ion | Collision energy(eV) |
|---------------------------|----------------------------|-----------------------------|-----------------------------|
| mono bromo | 260 [M] | 152.1 [-COBr] | 15 |
| | 262 [M] | 152.1 [-COBr] | 15 |
| di bromo | 339.9 [M] | 151.1 [-COBr ₂] | 20 |
| | 339.9 [M] | 180.1 [-Br ₂] | 20 |
| tri bromo | 417.8 [M] | 258 [-Br ₂] | 15 |
| | 419.8 [M] | 260 [-Br ₂] | 15 |
| tetra bromo | 497.8 [M] | 337.9 [-Br ₂] | 20 |
| | 337.9 [M-Br ₂] | 149.1 [-COBr ₂] | 45 |
| penta bromo | 575.7 [M] | 415.8 [-Br ₂] | 25 |
| | 415.8 [M-Br ₂] | 148.1 [-COBr ₃] | 55 |
| hexa bromo | 655.6 [M] | 495.7 [-Br ₂] | 20 |
| | 495.7 [M-Br ₂] | 335.8 [-Br ₂] | 30 |
| hepta bromo | 733.5 [M] | 573.6 [-Br ₂] | 25 |
| | 573.6 [M-Br ₂] | 305.7 [-COBr ₃] | 55 |
| octa bromo | 813.4 [M] | 653.6 [-Br ₂] | 25 |
| | 653.6 [M-Br ₂] | 545.7 [-COBr] | 30 |
| nona bromo | 891.3 [M] | 731.5 [-Br ₂] | 25 |
| | 731.5 [M-Br ₂] | 623.4 [-COBr] | 30 |
| deca bromo | 969.2 [M] | 809.4 [-Br ₂] | 25 |
| | 811.4 [M-Br ₂] | 651.5 [-Br ₂] | 50 |

Table 2. Optimised precursor and product ions for mono to deca brominated diphenyl ether ¹³C₁₂ labelled internal standards.

Figure 5 presents a calibration curve for the tetra bromo BDE#47, quantified against ¹³C₁₂-BDE#47, covering a concentration range of 1 to 400 pg on column, acquired on the 15 m DB1-HT GC Column. The calibration curve

gave a %RSD of 1.6%, demonstrating excellent linearity of response across this concentration range.

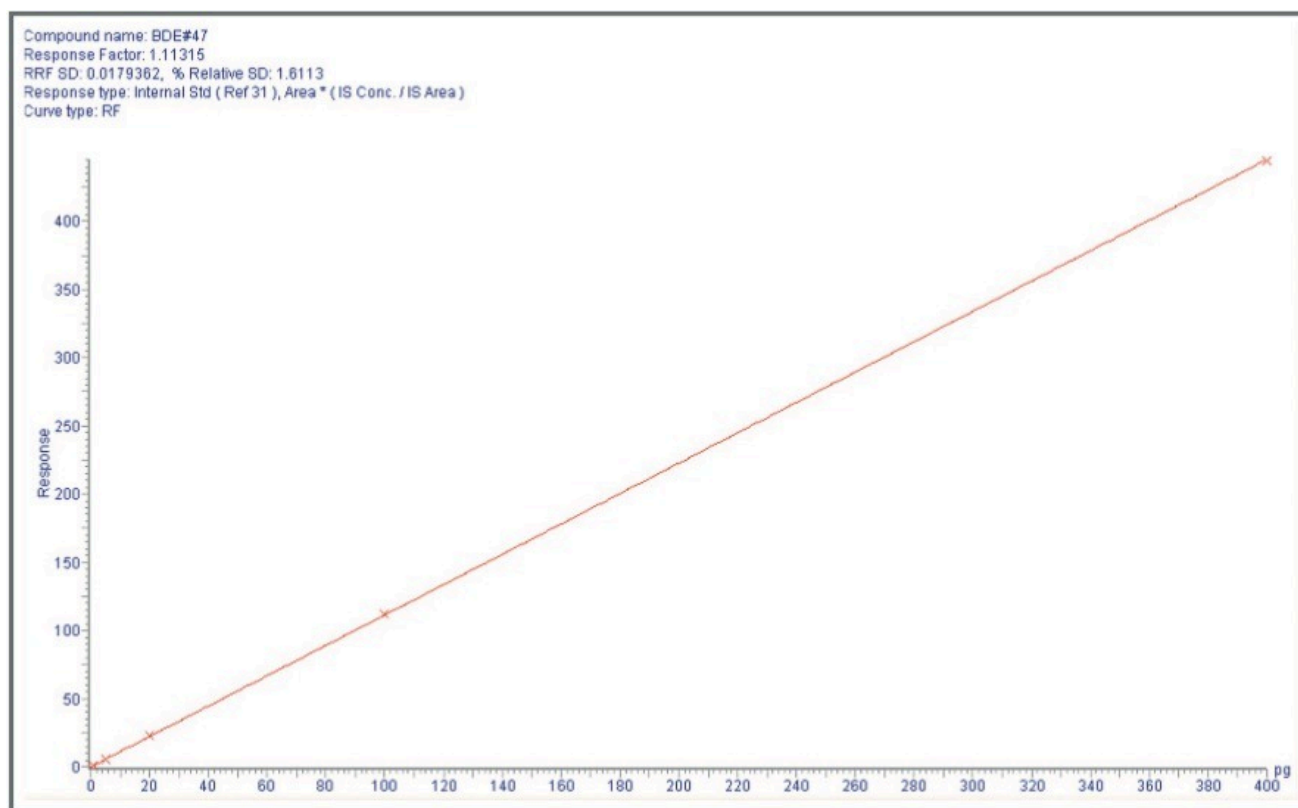


Figure 5. Calibration curve for tetra-bromo BDE#47, covering the concentration range 1–400 pg on column.

The limits of detection and quantification were calculated from the calibration curves acquired on each of the three GC columns. The DB5-ms Column was found to give the optimum separation of close eluting congener pairs, specifically the tetra brominated BDEs#49 and #71. However, the LOD and LOQ for the hexa-deca brominated BDEs were much higher using this column. Table 3 presents the calculated LOD values for each of the three columns for the 27 target BDE's, with all values calculated from acquiring all target peaks in a single injection.

| Name | 20m DB5-ms LOD (pg) | 15m DB1-HT LOD (pg) | 30m DB1-HT LOD (pg) |
|---------|------------------------|------------------------|------------------------|
| BDE#3 | 0.054 | 0.052 | 0.126 |
| BDE#7 | 0.054 | 0.053 | 0.099 |
| BDE#15 | 0.132 | 0.144 | 0.261 |
| BDE#17 | 0.069 | 0.08 | 0.137 |
| BDE#28 | 0.072 | 0.085 | 0.142 |
| BDE#49 | 0.152 | 0.154 | 0.189 |
| BDE#71 | 0.163 | 0.13 | 0.183 |
| BDE#47 | 0.144 | 0.133 | 0.177 |
| BDE#66 | 0.184 | 0.172 | 0.235 |
| BDE#77 | 0.696 | 0.587 | 0.771 |
| BDE#100 | 0.364 | 0.255 | 0.189 |
| BDE#119 | 0.41 | 0.248 | 0.198 |
| BDE#99 | 0.348 | 0.252 | 0.2 |
| BDE#85 | 0.919 | 0.582 | 0.459 |
| BDE#126 | 3.093 | 1.984 | 1.607 |
| BDE#154 | 0.686 | 0.349 | 0.316 |
| BDE#153 | 0.912 | 0.376 | 0.436 |
| BDE#138 | 1.352 | 0.534 | 0.494 |
| BDE#156 | 2.115 | 0.727 | 0.64 |
| BDE#184 | 1.141 | 0.394 | 0.439 |
| BDE#183 | 1.271 | 0.425 | 0.495 |
| BDE#191 | 2.129 | 0.563 | 0.706 |
| BDE#197 | 1.902 | 0.801 | 1.43 |
| BDE#196 | 3.275 | 0.974 | 1.885 |
| BDE#207 | 5.607 | 1.259 | 4.928 |
| BDE#206 | 18.243 | 2.082 | 9.711 |
| BDE#209 | 53.539 | 1.594 | 11.088 |

Table 3. Comparison of LODs in pg injected for the three GC columns employed.

As can be seen, the 15 m DB1-HT Column produced the best overall sensitivity, while maintaining a 50% valley between BDEs#49 and #71. Figure 6 shows the chromatographic separations obtained for the congeners BDE#49 and BDE#71 on the three GC columns used.

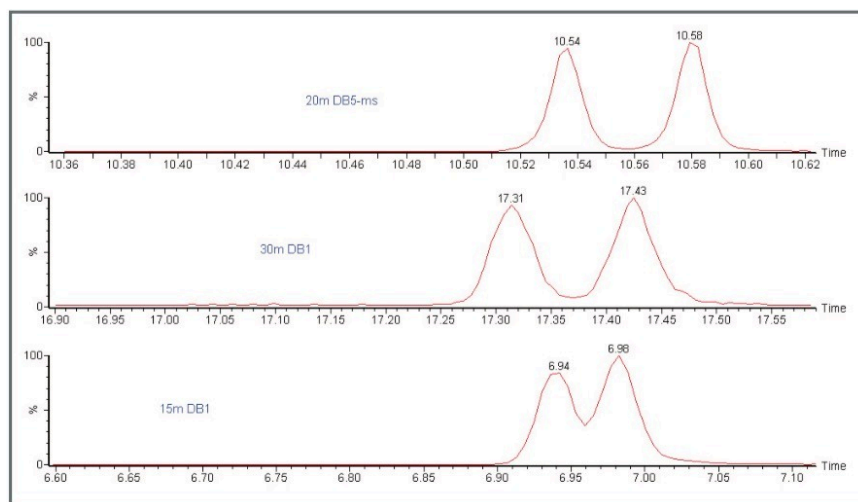


Figure 6. Comparison of the separation of BDE#49 and BDE#71 on the three GC columns used.

Figure 7 shows the chromatograms for tetra-bromo BDE#47 in a freeze-dried fish tissue extract, at a level of 150 ng/g dry weight. BDE#47 was detected in all of the samples at relatively high levels. The determined levels of the PBDEs were in good agreement with values obtained using high resolution GC-MS. Table 4 presents a comparison of the determined concentrations for BDE#47 in five sample extracts, quantified against the $^{13}\text{C}_{12}$ labelled BDE#47 internal standard. Table 5 presents a comparison of the determined concentrations for BDE#209 in five sample extracts, quantified against the $^{13}\text{C}_{12}$ labelled BDE#209 internal standard.

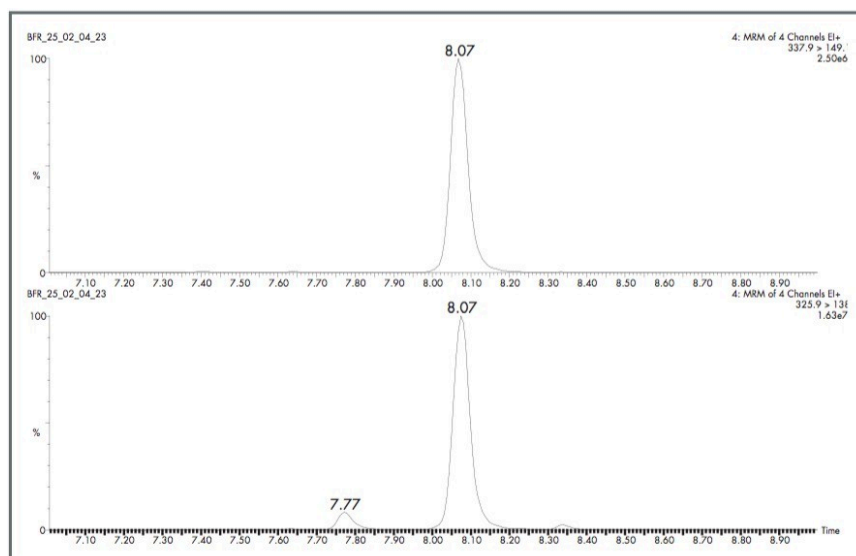


Figure 7. 139 ng/g BDE#47 (325.9>138) and its internal standard $^{13}\text{C}_{12}$ -BDE#47 (337.9>149.1) in a fish tissue extract.

| Matrix | GC-MSMS (ng/g) | HRGC-HRMS (ng/g) |
|----------------------------|----------------|------------------|
| Liquid stabilised biosolid | 482 | 530 |
| Liquid stabilised biosolid | 311 | 350 |
| dewatered biosolid | 435 | 490 |
| Fish tissue | 8.81 | 8.8 |
| Freeze dried fish tissue | 139 | 150 |

Table 4. Determined concentrations of BDE#47 in a variety of environmental matrices.

| Matrix | GC-MSMS (ng/g) | HRGC-HRMS (ng/g) |
|----------------------------|----------------|------------------|
| Liquid stabilised biosolid | 297 | 340 |
| Liquid stabilised biosolid | 264 | 290 |
| dewatered biosolid | 1630 | 1700 |
| Fish tissue | 0.32 | 0.4 |
| Freeze dried fish tissue | 0.4 | 0.3 |

Table 5. Determined concentrations of BDE#209 in a variety of environmental matrices.

Figure 8 shows the chromatograms for the quantification ion (799.3 > 639.5 transition) and confirmation ion (959.2 > 799.3 transition) for deca-brom BDE#209 in an air emission sample, at a level of 5.5 ng/m³.

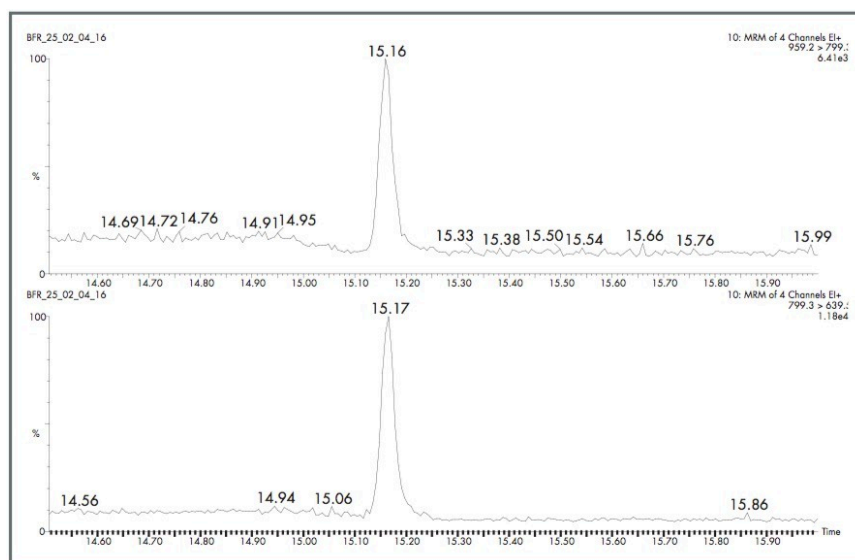


Figure 8. Deca-bromo BDE#209 in an air emission sample at a level of 5.5 ng/m³.

At the end of each acquisition sequence, the midpoint calibration standard BDE-CS3-E was injected, with its response compared with the five point calibration curve at the beginning of the sequence. Table 6 presents the results for analysis using the 15 m DB1-HT Column, for the calibration curve (mean RRF and RRF percentage

relative standard deviation), and the QC standard injection (percentage concentration deviation).

| Name | RRF Mean | % RSD | Daily check % deviation |
|---------|----------|-------|----------------------------|
| BDE#3 | 0.98 | 2.7 | -1 |
| BDE#7 | 3.2 | 1.9 | 3.9 |
| BDE#15 | 1.18 | 3.2 | 1.3 |
| BDE#17 | 1.32 | 4.6 | 6.3 |
| BDE#28 | 1.25 | 3.9 | 2.9 |
| BDE#49 | 0.96 | 1.3 | -6.2 |
| BDE#71 | 1.14 | 1.9 | 9.6 |
| BDE#47 | 1.11 | 1.6 | 2.3 |
| BDE#66 | 0.86 | 1.7 | -1.8 |
| BDE#77 | 0.25 | 4.1 | -9.2 |
| BDE#100 | 1.03 | 3.7 | 0.9 |
| BDE#119 | 1.06 | 2.4 | 4.2 |
| BDE#99 | 1.04 | 6.5 | -3.6 |
| BDE#85 | 0.45 | 2.9 | -3.1 |
| BDE#126 | 0.13 | 4 | -6.5 |
| BDE#154 | 1.01 | 4.1 | 4 |
| BDE#153 | 0.83 | 1.6 | -1.6 |
| BDE#138 | 0.66 | 7.5 | -6.4 |
| BDE#156 | 0.48 | 10.3 | -9.9 |
| BDE#184 | 0.91 | 2.2 | 2.2 |
| BDE#183 | 0.85 | 3.3 | 1.8 |
| BDE#191 | 0.64 | 3 | -6.1 |
| BDE#197 | 0.96 | 4.7 | -1.4 |
| BDE#196 | 0.79 | 6.6 | -9.3 |
| BDE#207 | 0.76 | 3.6 | -2.5 |
| BDE#206 | 0.46 | 13.7 | -4.2 |
| BDE#209 | 1.22 | 1.9 | 1.5 |

Table 6. Calibration curve and calibration check standard results, using the 15 m DB1-HT GC Column.

As can be seen, the calibration %RSD values are all <15%, and the response deviations are all <10%, showing the excellent linearity and stability of response offered by a triple quadrupole mass spectrometer.

Conclusion

GC triple quadrupole MS provides a sensitive and easy to apply method for the analysis of brominated diphenyl ether flame retardants, offering a rapid analysis time whilst providing suitable confirmation of analyte presence. The fragmentation of PBDEs in the collision cell allows specific MRM transitions to be monitored for each level of bromination, giving a high degree of selectivity. The use of a 15 m DB1-HT GC Column allowed good LOD/LOQ values to be obtained for all target peaks, at the expense of poorer separation of some congener pairs. The optimum method for the quantification of mono-deca brominated PBDEs would be the use of a 15 m DB1-HT Column for hepta-deca brominated congeners, and a DB5-ms Column for the determination of mono-hexa brominated PBDEs.

References

1. USA Today, 23rd September 2003.
2. Usukura, K; Seko, T and Onda, N. Japan Society for Analytical Chemistry *Analytical Sciences* 2001; 17; 579–580.
3. Kuhn, E; Ellis, J; Prest, H; Trainor, T and Gelbin, A. *Organohalogen Compounds* 2003; 61; 139–142.
4. Larrazabal, D; Martinez; M.A. and Fabrellas, B. *Organohalogen Compounds* 2003; 61; 57–60.

720001021, October 2004

© 2022 Waters Corporation. All Rights Reserved.